

# Numerical investigation of mixing in serpentine microchannels

Nishit Pachpande

BITS Pilani, K.K. Birla Goa Campus  
FOSSEE Mentor: Mr. Binayak Lohani

Supervisor: Dr. P. R. Naren,  
SASTRA Deemed to be University, Thanjavur, Tamil Nadu.

## Abstract

A numerical model is developed in order to study the extent of mixing of fluids in serpentine microchannel, and a parametric study involving geometric and physical parameters like waviness of the micromixer ( $\alpha$ ), wavelength of the micromixer ( $\gamma$ ), Reynolds Number ( $Re$ ). Two-dimensional numerical model was developed in OpenFOAM, version 2012 and grid sensitivity analysis was performed. Further, simulations were done on the grid independent mesh at various operating conditions and geometric parameters. The work is also validated with the Mondal *et al.* 2019 study. Pressure drop, tracer concentration and velocity contours were studied for Reynolds numbers of 1, 5, 25, 50 and 100.

## 1 Introduction

### 1.1 Aim

The study aims to determine the extent of mixing of fluids in serpentine microchannels, with varying geometric parameters. Study of mixing of fluids at a micro scale has become one of the latest topics of research due to its wide applications in lab-on-chip devices, medical diagnostics, drug delivery, micro-reactors etc. As viscous forces are dominant at a micro scale, the flow through such devices is laminar in nature. Furthermore, very low magnitude of diffusivity of fluids results in very slow mixing. Thus, design and analysis of microfluidic devices is required for efficient mixing. A “T” shaped tree type structure is preferred by researchers as a passive micro-mixer design, as stated in the Mondal *et al.* 2019 study.

### 1.2 Problem Statement and objectives of the study

The primary objective of this study is to determine the mixing of fluids by studying the velocity, pressure and tracer concentration contours and pressure drop of fluid passing through the micro-

mixer. The study numerically analyzes characteristics of flow for serpentine micro-mixer at various lower Reynolds numbers 1, 5, 25, 50, 100 and Schmidt number of 100.

The numerical model is developed and has been verified on the basis of the works of Mondal *et al.* 2019 study on serpentine and racoon micromixers. Mondal *et al.* 2019 study has analyzed flow characteristics for two micromixer configurations- serpentine and racoon micromixers, for different magnitudes of waviness( $\alpha$ ), wavelength of waviness( $\lambda$ ), Reynolds number( $Re$ ) and Schmidt number( $Sc$ ).

## 2 Methodology

### 2.1 Geometry

#### 2.1.1 Geometry specifications

The serpentine microchannel employed in the current work is shown in the figure 1. The fluid enters the domain at a uniform velocity through two inlets-Inlet 1, Inlet 2, which mixes along the serpentine channel and exits from the outlet. The inlet width ( $L$ ) has a magnitude of  $150\mu\text{m}$ . Table 1 defines all of the geometric parameters used in the study.

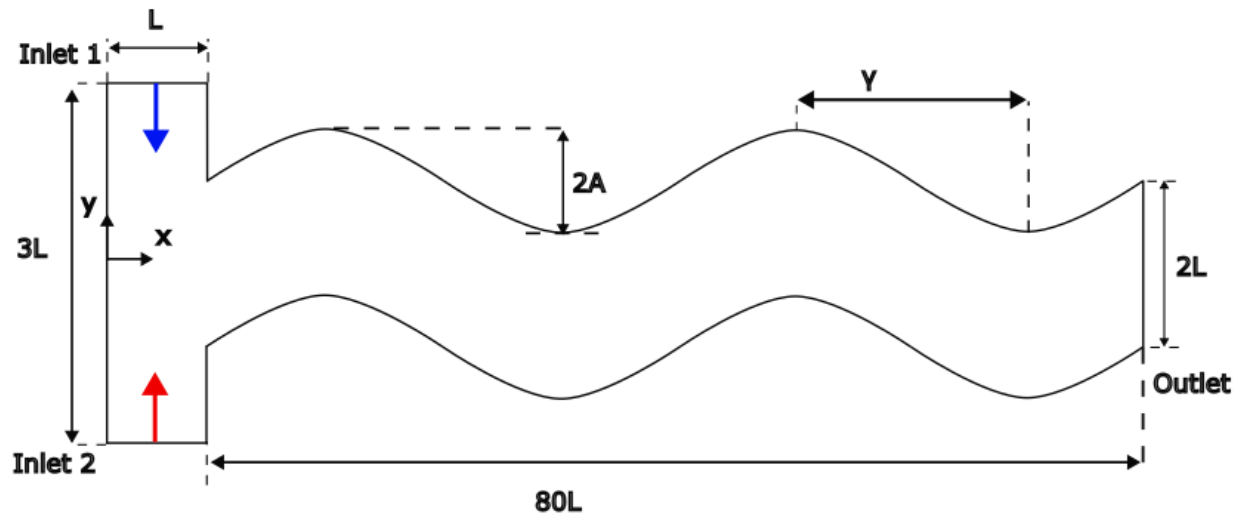


Figure 1: Serpentine microchannel geometry (Mondal *et al.* 2019.)

For the serpentine microchannel, the equation of the wavy profile for the top wall is given by:

$$S(x) = -L + A\sin(2\pi(x - L)/\gamma)$$

Similarly, for the bottom wall:

$$S(x) = -L + A\sin(2\pi(x - L)/\gamma + \pi)$$

Symbol	Geometric significance
A	Amplitude of waviness, m
L	Inlet Width, m
$\alpha$	Dimensionless amplitude of sinusoidal geometry (= A/L)
$\gamma$	Wavelength of sinusoidal geometry, m
$\lambda$	Dimensionless wavelength of sinusoidal geometry (= $\gamma/L$ )

Table 1: Geometry Nomenclature

### 2.1.2 Meshing

The geometry modelling and grid generation has been done on Gmsh software of version 4.11.1. Geometry has been modelled keeping in mind the parametric study that needs to be performed by varying the amplitude and wavelength of the microchannel. Hence, the study is done for  $\alpha$  values of 0.15, 0.3 and 0.45 and  $\lambda$  values of 4, 8 and 12.

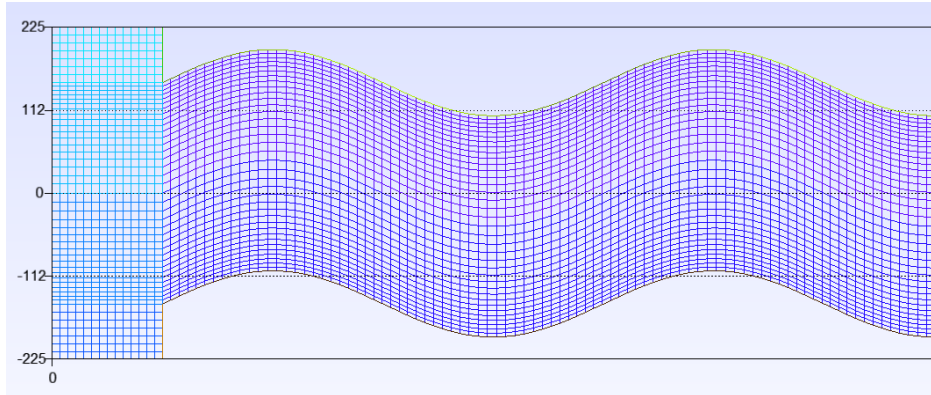


Figure 2: Meshed Geometry for  $\alpha = 0.3$  and  $\lambda = 4$ . (Max. skewness of 0.483 and Max aspect ratio of 4.08)

## 2.2 Governing Equations

For this study, a two-dimensional, steady, laminar, incompressible flow of Newtonian fluid has been considered. Following are governing equations for the model, and gravity has been neglected in the study:

Continuity Equation:

$$\frac{\partial u}{\partial x} + \frac{\partial v}{\partial y} = 0$$

x-momentum equation:

$$\rho \left( u \frac{\partial u}{\partial x} + v \frac{\partial u}{\partial y} \right) = -\frac{\partial p}{\partial x} + \mu \left( \frac{\partial^2 u}{\partial x^2} + \frac{\partial^2 u}{\partial y^2} \right)$$

y-momentum equation:

$$\rho \left( u \frac{\partial v}{\partial x} + v \frac{\partial v}{\partial y} \right) = -\frac{\partial p}{\partial y} + \mu \left( \frac{\partial^2 v}{\partial x^2} + \frac{\partial^2 v}{\partial y^2} \right)$$

Mass Transport Equation:

$$u \frac{\partial c}{\partial x} + v \frac{\partial c}{\partial y} = D \left( \frac{\partial^2 c}{\partial x^2} + \frac{\partial^2 c}{\partial y^2} \right)$$

## 2.3 Boundary Conditions

The following boundary conditions are applied for solving the case. Two similar fluids, with similar properties and velocity, are introduced at the two inlets-“Inlet1” & “Inlet2”. Water, with a density of  $1000 \text{ kg/m}^3$  and kinematic viscosity  $10^{-6} \text{ m}^2/\text{s}$  has been considered as the working fluid.

No-slip boundary condition has been applied at the walls of the microchannel. A tracer is introduced at inlet-2 throughout the simulation. Therefore, the dye concentration “T” at inlet-1 & inlet-2 is 0 & 1 respectively. Figure 3 depicts the boundary conditions applied on the geometry, where T is the tracer concentration and U is the uniform velocity at both of the inlets.

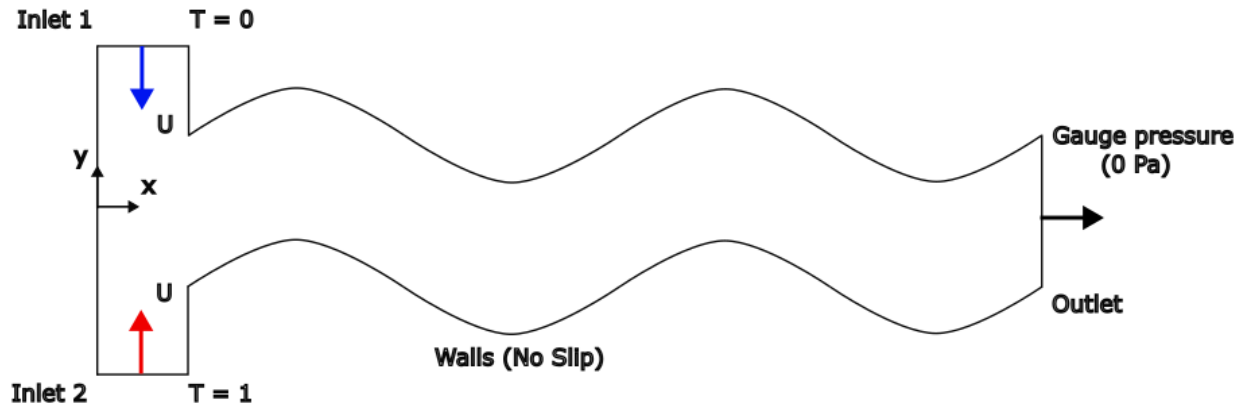


Figure 3: Boundary Conditions

## 2.4 Solving Setup

The imported mesh with the applied boundary conditions is further solved using Semi-Implicit Method for Pressure-Linked Equations (SIMPLE) algorithm for Reynolds numbers 1,5,25,50,100, for the continuity and momentum equations. Additionally for solving the mass transport equation, the two solvers of OpenFOAM- simpleFoam and scalarTransportFoam were combined.

Central Differencing scheme was preferred due to its second order property. Generalized Geometric-Algebraic MultiGrid (GAMG) solver was used for solving pressure and tracer concentration. Symmetric Gauss Seidel solver was used for velocity. The residual tolerances for p, T(tracer concentration) and U were set to be  $10^{-6}$ ,  $10^{-6}$  and  $10^{-5}$  respectively.

The solution was iterated till convergence is attained, and the pressures and velocities at inlets and outlet were observed at each iteration, to ensure that convergence is reached. A subroutine was defined in controlDict file to note the area averaged pressure and velocity at a given plane at the end of each iteration. The subroutine is presented as follows:

```

surfaceFieldValue1
{
    // Mandatory entries (unmodifiable)
    type                surfaceFieldValue;
    libs                (fieldFunctionObjects);

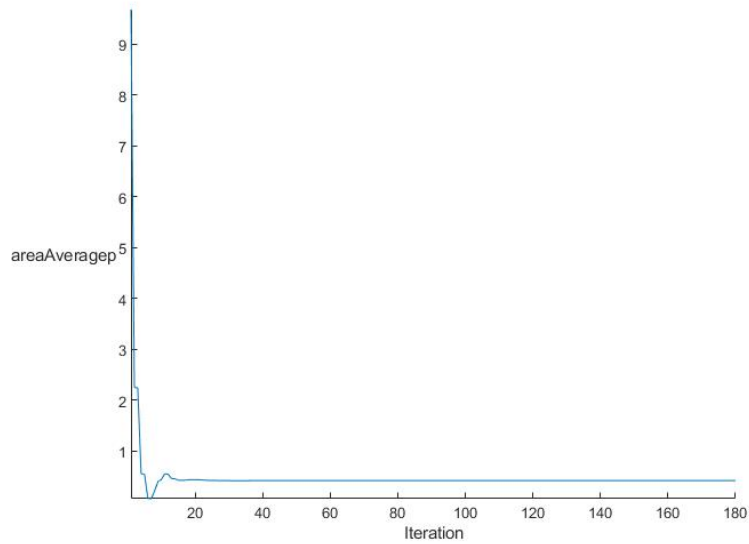
    // Mandatory entries (runtime modifiable)
    fields              (p U);
    operation           areaAverage;
    regionType          patch;
    name                inlet1;

    // Optional entries (runtime modifiable)
    postOperation       none;
    weightField         alpha1;
    scaleFactor         1.0;
    writeArea           false;
    surfaceFormat       none;

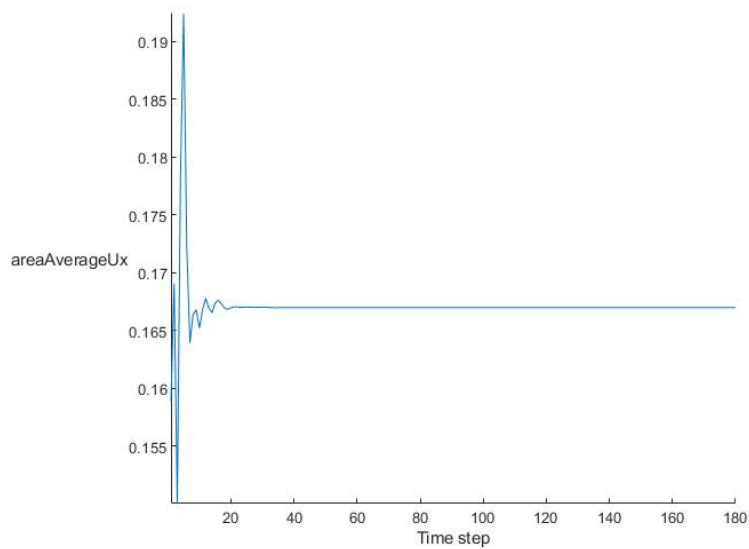
    // Optional (inherited) entries
    writeFields         false;
    scalingFactor       1.0;
    writePrecision      8;
    writeToFile         true;
    useUserTime         true;
    region              region0;
    enabled             true;
    log                 true;
    timeStart           0;
    timeEnd             1000;
    executeControl      timeStep;
    executeInterval     1;
    writeControl        timeStep;
    writeInterval       1;
}

```

The area averaged pressures and velocities at the inlet and the outlet is recorded at each iteration and is shown in Fig 4. It is observed from the figure that simulation is converged as there is no significant change in the magnitude of area weighted average pressure and velocity with iteration. Hence, it is verified that the solution attains steady state condition, as depicted the figure below. With the set solver conditions, cases were simulated with lower Reynolds numbers of 1, 5, 25, 50 & 100 and a Schimidt number of 100, for the geometric parameter of  $\alpha = 0.3$  and  $\lambda = 4$ .



(a) Area averaged pressure at inlet vs time step



(b) Area averaged velocity at outlet vs time step

Figure 4: Steady state validation for Reynolds number 25 and Schmidt number 100

### 3 Results and Discussions

After the solution was converged, the post-processing was carried out on Paraview 5.11.0. Tracer concentration and velocity contours and pressure drops from each case were noted.

### 3.1 Mesh sensitivity analysis

Grid sensitivity analysis has been performed for  $\alpha = 0.3$  and  $\lambda = 4$ . Table 2 shows the absolute percentage error in pressure drops for the meshes M1, M2 and M3. Figure 2 illustrates the Mesh

Mesh	Number of Elements	% error
M1	41,260	0.78
M2	75,426	0.45
M3	149,938	-

Table 2: Grid sensitivity

M2 for geometric configuration of  $\alpha = 0.3$  and  $\lambda = 4$ . Mesh M2 is utilized for further numerical simulations with a maximum skewness of 0.483 and maximum aspect ratio of 4.08.

### 3.2 Pressure Drop

Pressure Drop was calculated from difference between area averaged pressure at inlet and outlet (0 Pa). The area averaged pressures were obtained from surfaceFieldValue0 function defined in controlDict file. Table 3 illustrates pressure drop at Reynolds numbers 1, 5, 25, 50 & 100. The

Reynolds Number	Pressure drop (Pa)
1	13.86
5	71.38
25	411.48
50	925.92
100	2215.18

Table 3: Calculated pressure drop at Reynolds numbers 1, 5, 25, 50 & 100

Below figure shows the calculated pressure drop and Mondal *et al.* 2019 pressure drop vs the Reynolds numbers- 1, 5, 25, 50 & 100. It is observed that the present work could successfully capture the trend as reported by Mondal *et al.* 2019.

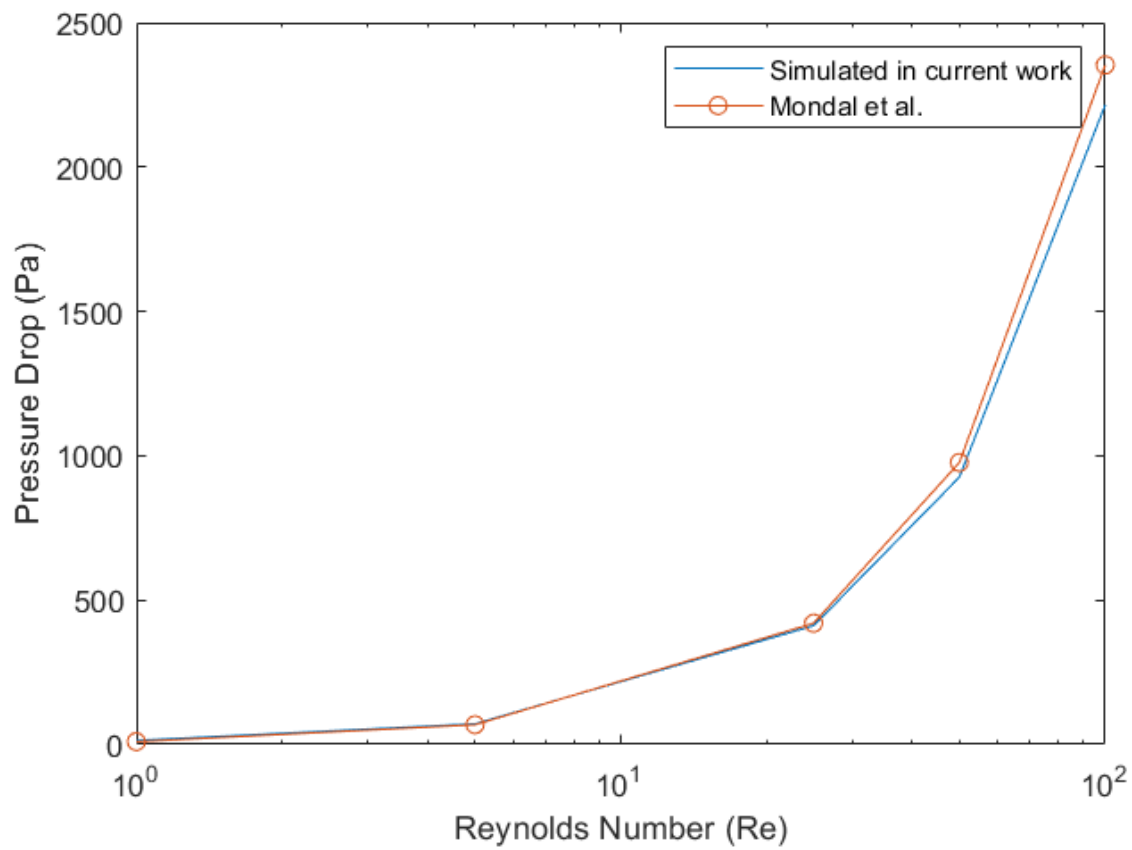


Figure 5: Calculated pressure drop & Mondal *et al.* 2019 pressure drop at various Reynolds numbers for  $\alpha = 0.3$  &  $\gamma = 4$



### 3.3 Tracer concentration contours

Tracer concentration contours at Reynolds numbers 1, 5, 25, 50 & 100 is shown below. The contours are given for the geometric parameter of  $\alpha = 0.3$  &  $\gamma = 4$ .

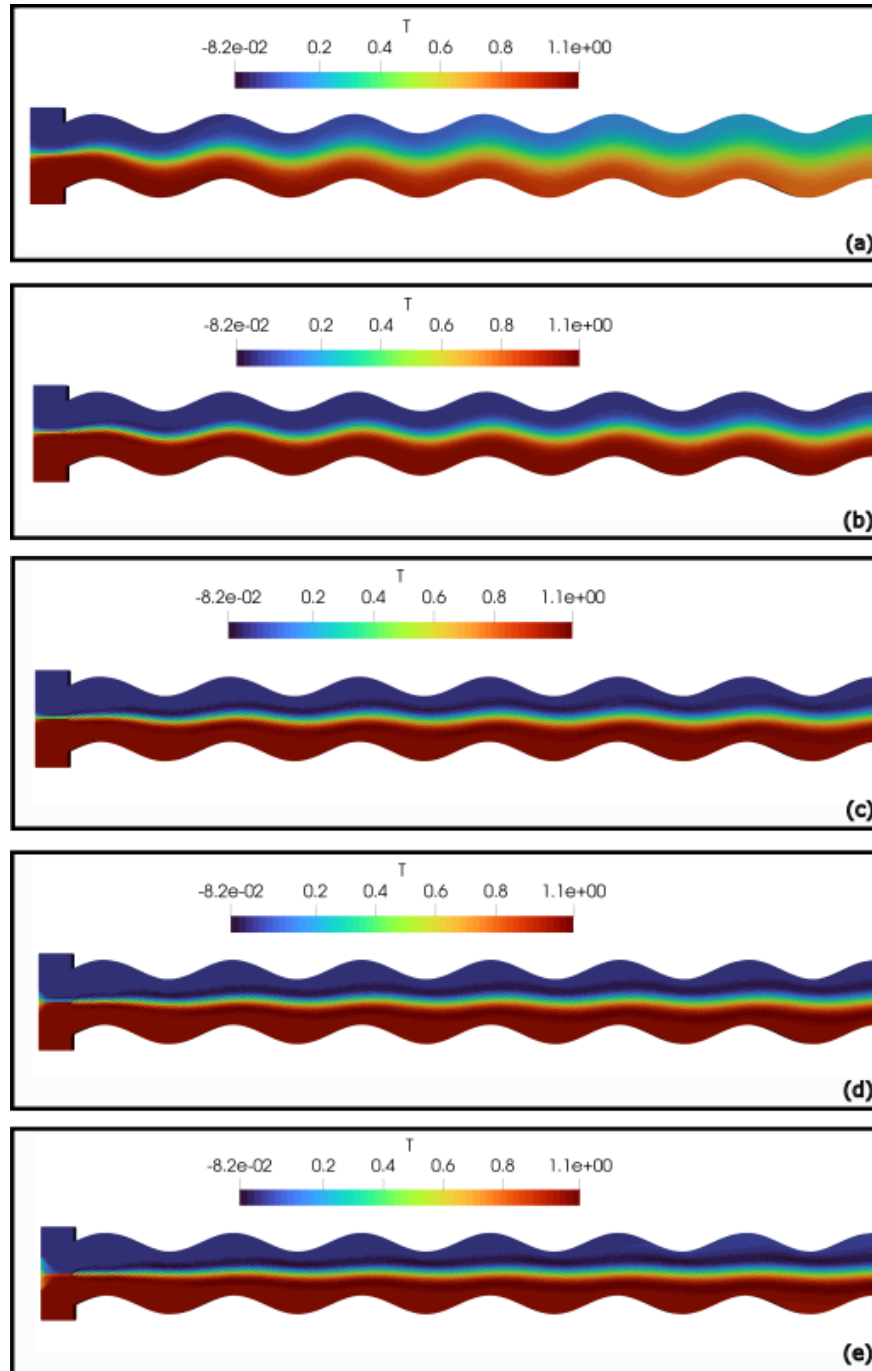


Figure 6: Tracer Concentration contours for  $\alpha = 0.3$  &  $\gamma = 4$  at (a)  $Re = 1$ , (b)  $Re = 5$ , (c)  $Re = 25$ , (d)  $Re = 50$  and (e)  $Re = 100$ .

### 3.4 Velocity contours

Velocity contours at Reynolds numbers 1, 5, 25, 50 & 100 is shown below, for the geometric parameter of  $\alpha = 0.3$  &  $\gamma = 4$ .

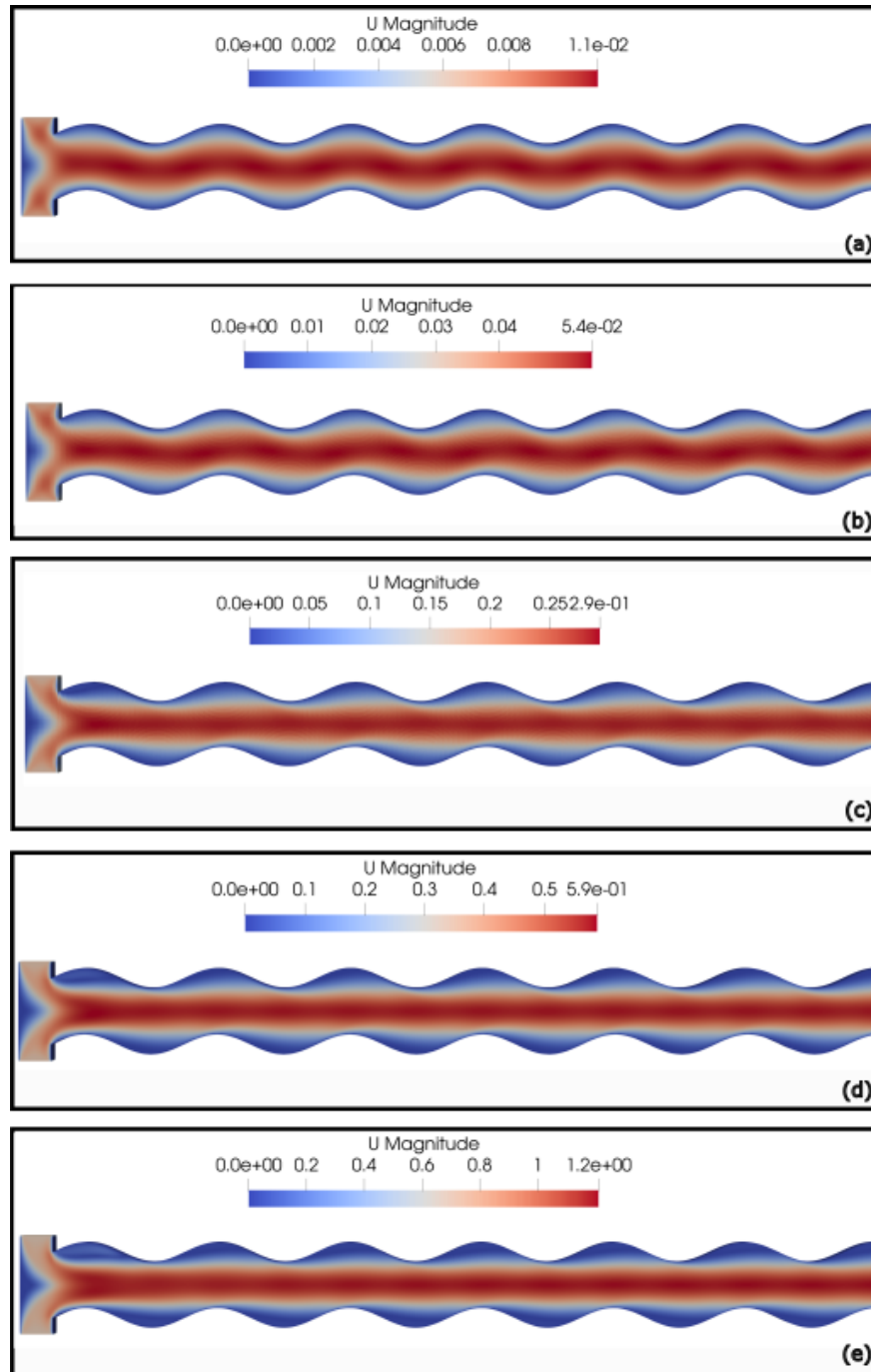


Figure 7: Velocity contours for  $\alpha = 0.3$  &  $\gamma = 4$  at (a)  $Re = 1$ , (b)  $Re = 5$ , (c)  $Re = 25$ , (d)  $Re = 50$  and (e)  $Re = 100$ .

The tracer concentration and velocity contours above were found to be similar to the contours

in Mondal *et al.* 2019 study for serpentine channel of  $\alpha = 0.3$  &  $\gamma = 4$  and at Reynolds numbers 1, 5, 25, 50, & 100 (See Figure 7 of Mondal *et al.* 2019).

## 4 Summary

Numerical studies have been conducted to study the extent of mixing by adding curviness to the typical microchannels, which have been named as serpentine microchannels. Geometry and meshing was done on Gmsh version 4.11.1. A custom solver was implemented to solve for the continuity, momentum and mass-transport equations, on OpenFOAM 2012.

Grid sensitivity analysis was conducted to ensure use of optimal number of cells. The Pressure drop across the inlet and outlet, tracer concentration contours, velocity contours were studied using post processing software Paraview 5.11.0. From the pressure drop calculations, it can be inferred that the pressure drop values were close to the values from Mondal *et al.*'s study. One notable observation is that the pressure drop has an increasing trend with increase in the Reynolds number, which means a higher pumping power is required for high Reynolds numbers.

## 5 Further Work

The work can be extended to studying mixing at different wavelengths and amplitudes. Currently, the model has been solved with geometric configuration of  $\alpha = 0.3$  &  $\gamma = 4$ . Furthermore, Residence time distribution (RTD) study can be conducted, wherein tracer can be introduced as a step function with time, and transient studies can be done.

## 6 Notations

c	Tracer/Dye concentration ( $\text{molm}^{-3}$ )
D	Diffusion coefficient of species ( $\text{m}^2\text{s}^{-1}$ )
p	Pressure (Pa)
u	x velocity component ( $\text{ms}^{-1}$ )
v	y velocity component ( $\text{ms}^{-1}$ )
x	Axial distance (m)
y	Transverse distance (m)

Greek symbols:

$\mu$	dynamic viscosity ( $\text{kgm}^{-1}\text{s}^{-1}$ )
-------	--

## 7 References

- Mondal, B., Mehta, S., Patowari, P., Pati, P.(2019). Numerical study of mixing in wavy micromixers: comparison between raccoon and serpentine mixer. *Chemical Engineering and Processing - Process Intensification*, 136:44-61.